Supporting Information

Violet Phosphorus Quantum Dots as an Emerging Visible light-responsive Photocatalyst for Efficient Hydrogen Evolution Reaction

Xin Wang,[a] Chang Xu,[b] Ziyou Wang,[a] Yan Wang,[a] Xuewen Zhao,[c] Jinying Zhang,[c] Ming Ma,[a] Quansheng Guo[b] and Fuxiang Zhang*[d]*

[a] X. Wang, Z. Wang, Y. Wang, M. Ma
Shenzhen Institute of Advanced Technology
Chinese Academy of Sciences
Shenzhen, 518055, China
E-mail: xin.wang2@siat.ac.cn

[b] C. Xu, Q. Guo
School of Materials Science and Engineering
Hubei University
Wuhan, 430062, China

[c] X. Zhao, J. Zhang
State Key Laboratory of Electrical Insulation and Power Equipment
Center of Nanomaterials for Renewable Energy
School of Electrical Engineering, Xi'an Jiaotong University
Xi'an, Shaanxi, 710049, China

[d] F. Zhang
State Key Laboratory of Catalysis
Dalian Institute of Chemical Physics
Chinese Academy of Sciences
Dalian 116023, China
E-mail: fxzhang@dicp.ac.cn

Results and Discussion

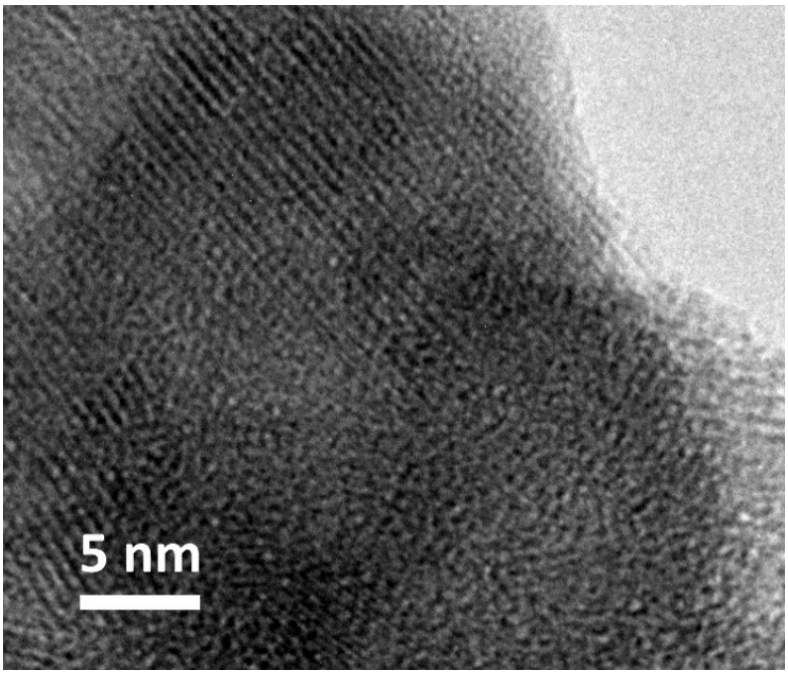

Fig. S1. HRTEM image of VP crystals.

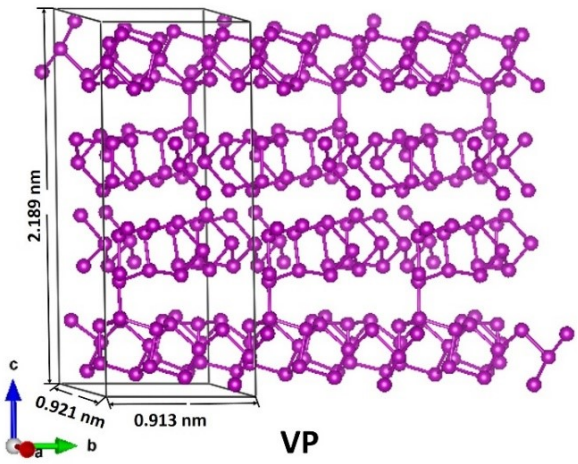

a-axis	b-axis	c-axis
0.921 nm	0.913 nm	2.189 nm
α	β	γ
90.0 °	97.8 °	90.0 °

Fig. S2. The crystal structure of VP shown using ball-and-stick models and the corresponding unit cell parameters. The crystal structures were visualized using the VESTA suite of programs.[1]

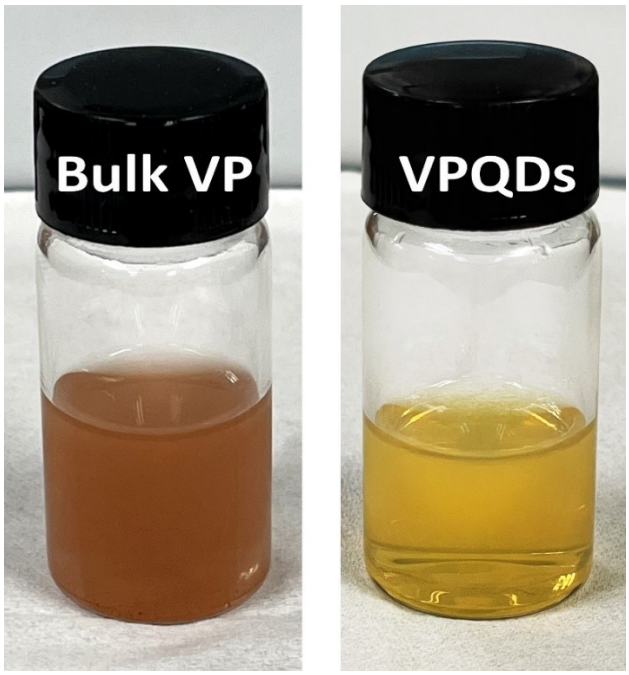

Fig. S3. Photographs of bulk VP and VPQDs dispersion.

Table S1 Yields of VPQDs obtained after centrifugation at 3K rpm for 20 min.

Sample	m_0[1] (mg)	m_g[2] (mg)	Δm[3] (mg)	Yield (%)
A	10.24	6.83	3.41	33.30%
B	15.18	10.50	4.68	30.83%
C	20.36	14.22	6.14	30.15%

[1]*m_0 is the mass of the initial VP crystals.*

[2]*m_g is the mass of the solid product after centrifugation at 3K rpm for 20 min.*

[3]*Δm is the mass of the VPQDs product, calculated from the equation $\Delta m = m_0 - m_g$.*

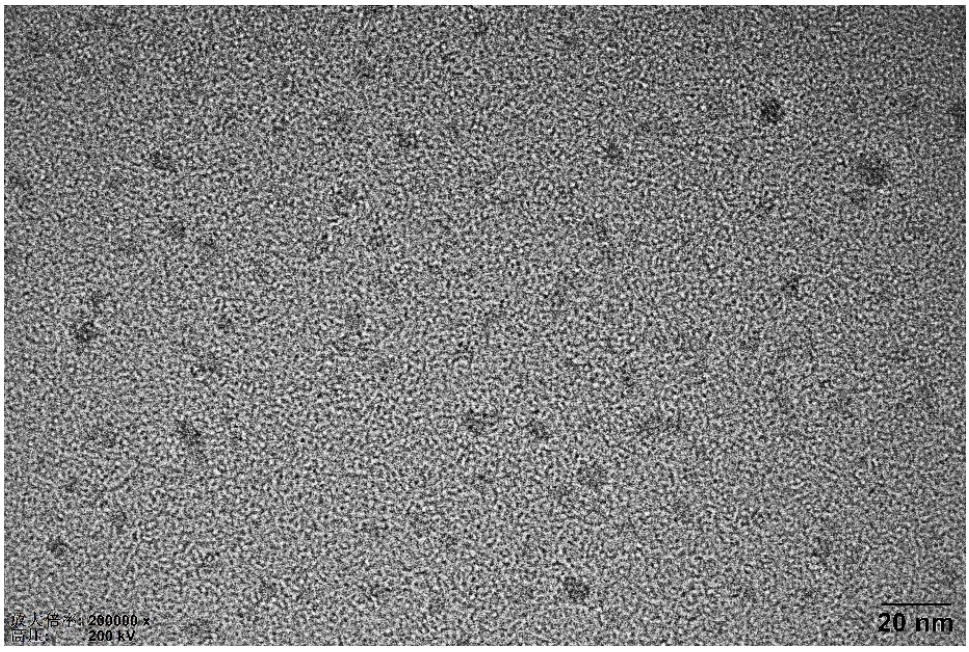

Fig. S4. The magnified TEM image of VPQDs.

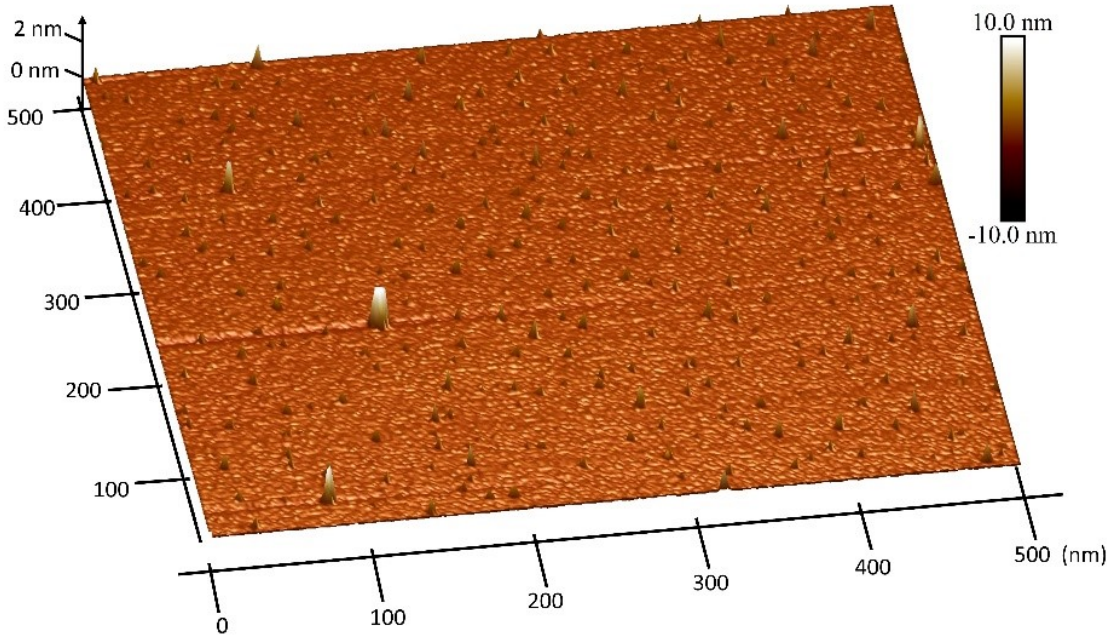

Fig. S5. 3D AFM topography of the as-prepared VPQDs.

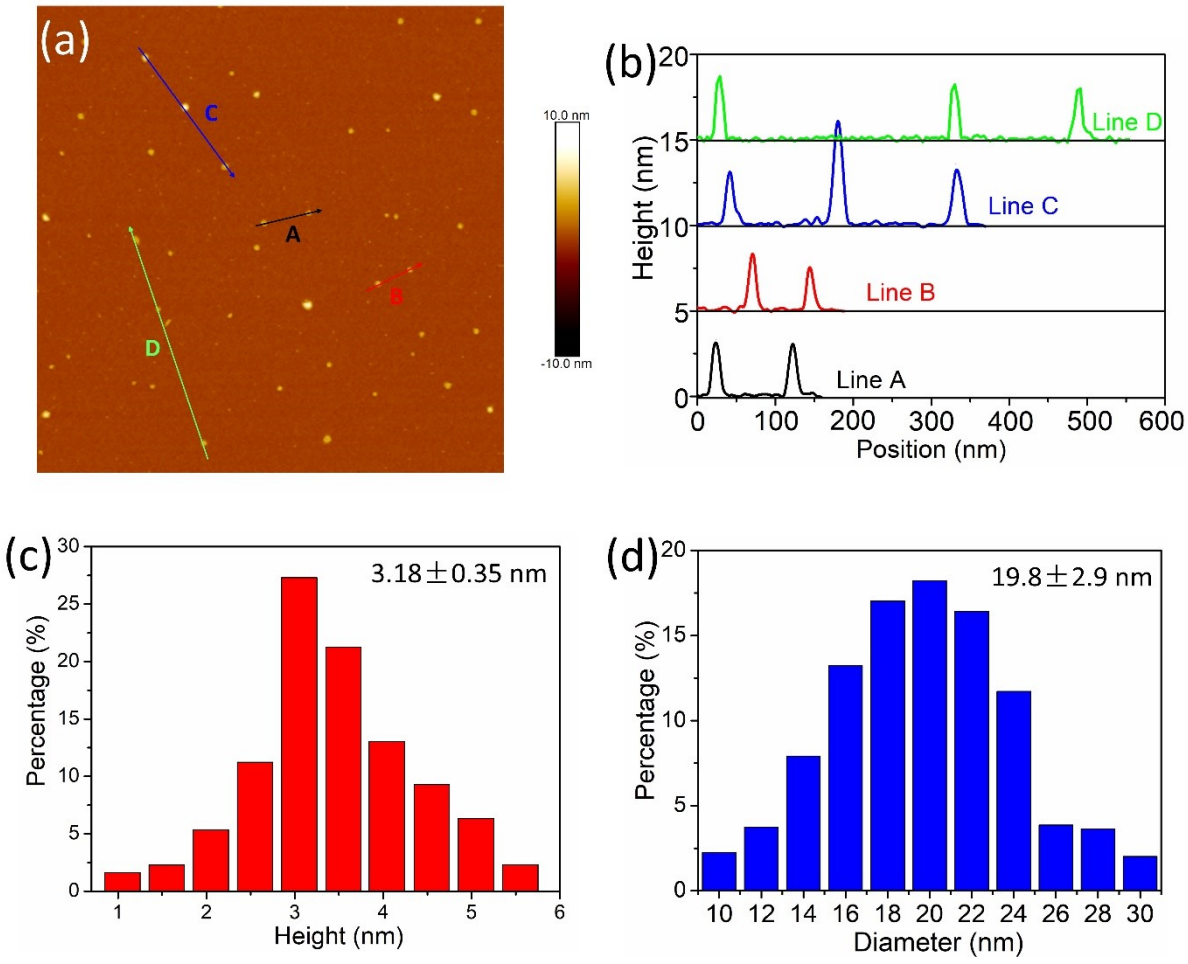

Fig. S6. (a) AFM images of VPQDs obtained at centrifugation ranges of 7-9 k. (b) Height profiles along line A, line B, line C and line D in a. (c) Statistical analysis of the heights of VPQDs measured by the AFM image in a. (d) Statistical analysis of the lateral sizes of VPQDs measured by the AFM image in a.

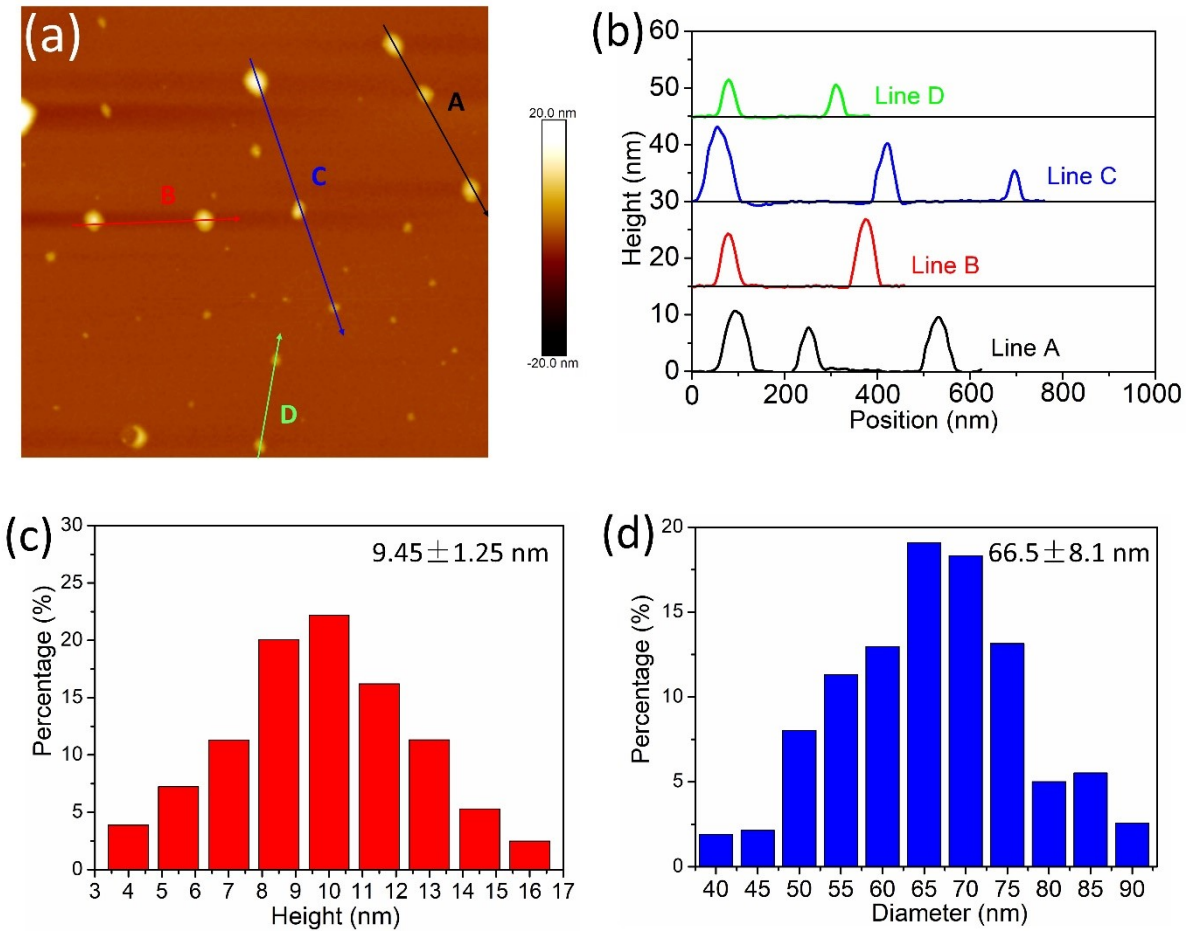

Fig. S7. (a) AFM images of VPQDs obtained at centrifugation ranges of 5-7 k. (b) Height profiles along line A, line B, line C and line D in a. (c) Statistical analysis of the heights of VPQDs measured by the AFM image in a. (d) Statistical analysis of the lateral sizes of VPQDs measured by the AFM image in a.

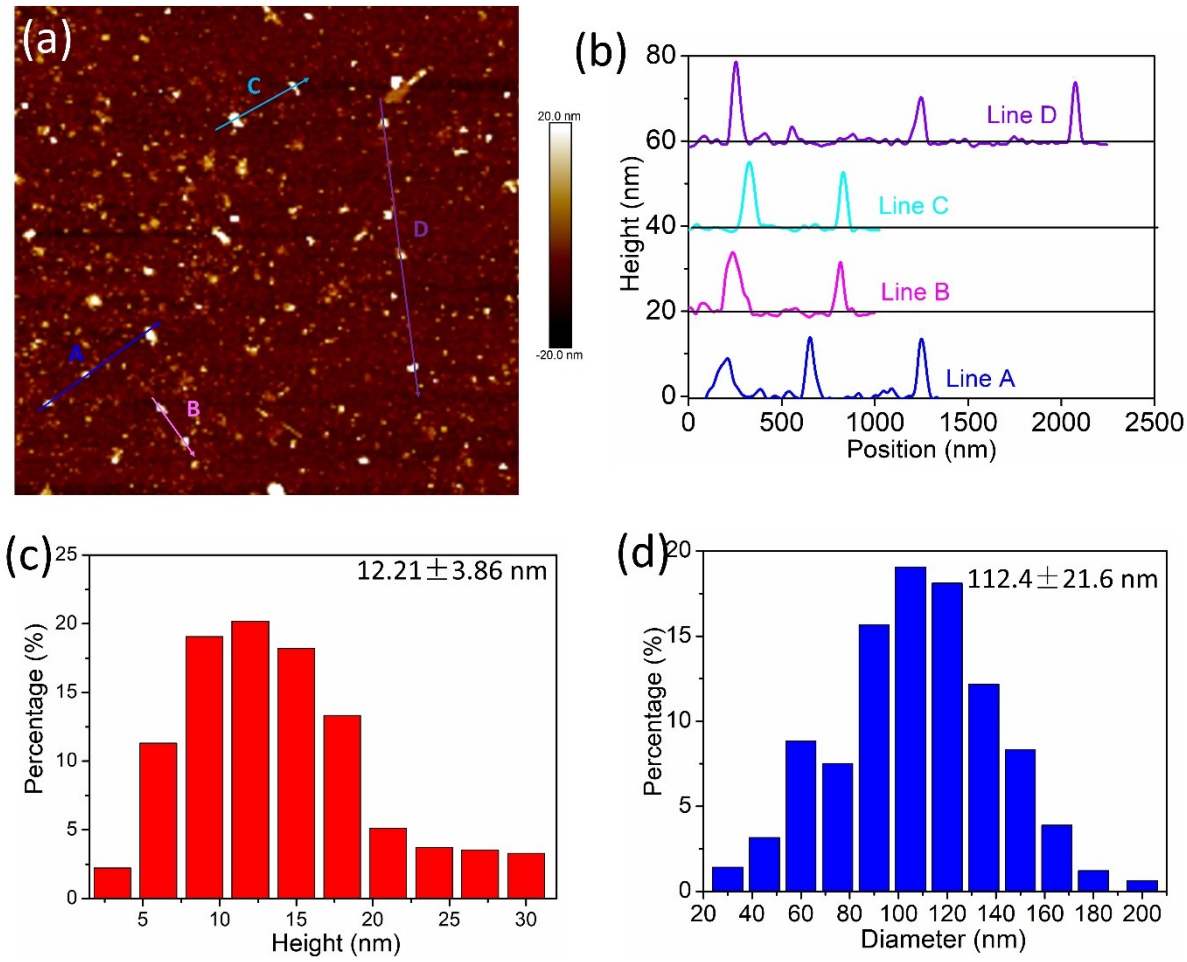

Fig. S8. (a) AFM images of VPQDs obtained at centrifugation ranges of 3-5 k. (b) Height profiles along line A, line B, line C and line D in a. (c) Statistical analysis of the heights of VPQDs measured by the AFM image in a. (d) Statistical analysis of the lateral sizes of VPQDs measured by the AFM image in a.

XPS spectra

Fitting analysis shows that the P 2p peaks can be deconvoluted into five peaks at 129.6, 130.5, 131.7, 133.4 and 134.5 eV. The peaks at 129.6 and 130.5 can be assigned to P $2p_{3/2}$ and P $2p_{1/2}$ of the P=P bonds. Moreover, the peaks at 131.7, 133.7, and 134.5 eV can be ascribed to the oxidized phosphorus of P-O-P (bridging bonding), O-P=O (dangling bonding) and P_2O_5, respectively.[2-4]

Table S2. The intensity ratio of P_xO_y to P=P in the XPS spectra of the bulk VP and VPQDs.

Samples	P_xO_y	P=P	P_xO_y/P=P
VP	45.8	54.2	0.845
VPQDs	27.7	72.3	0.383

Raman spectra

Raman Microscopy was performed using a Thermo DXR 2xi Raman spectrometer equipped with excitation wavelengths of 514 nm. Three prominent peaks at 353, 446 and 471 cm^{-1} were detected for both bulk VP and VPQDs, respectively. Among them, the Raman features at 353 cm^{-1} is ascribed to the stretching vibrational modes of [P9] cages ($S^2_{[P9]}$) and the Raman feature at 471 cm^{-1} is due to the tangential stretching mode of [P9] along the tubular axis (Tg). Moreover, the intensity ratio of $S^2_{[P9]}$ to T_g was observed to change from 0.68 (bulk VP) to 0.77 (VPQDs) indicating the successful synthesis of VPQDs since the stretching vibrational modes of [P9] are affected by the surrounding molecules more significantly than the tangential stretching mode of [P9] along the tubular axis after quantum size effects.[5-7]

Table S3. The intensity ratio of $S^2_{[P9]}$ to T_g in the Raman spectra of VP and VPQDs.

Samples	$S^2_{[P9]}$	T_g	$S^2_{[P9]}/T_g$
VP	1120.2	1640.1	0.68
VPQDs	979.1	1264.1	0.77

Table S4. The band positions as well as the work functions of VPQDs and the bulk VP.[8,9]

Samples	E ($_{bandgap}$)	E_{VB}(Vs vacuum)	E_{VB} (Vs.NHE)	E_{CB} (Vs.NHE)	Work functions (ϕ)
Bulk VP	1.88	6.11	1.67	-0.21	4.9
VPQDs	2.06	6.16	1.72	-0.34	4.65

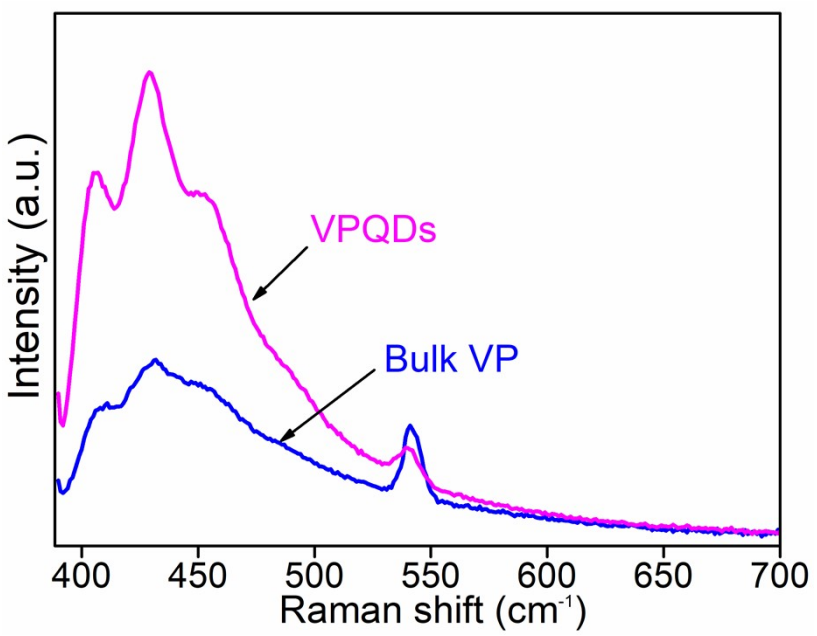

Fig. S9. Steady-state PL emission spectra of VPQDs and the bulk VP crystals.

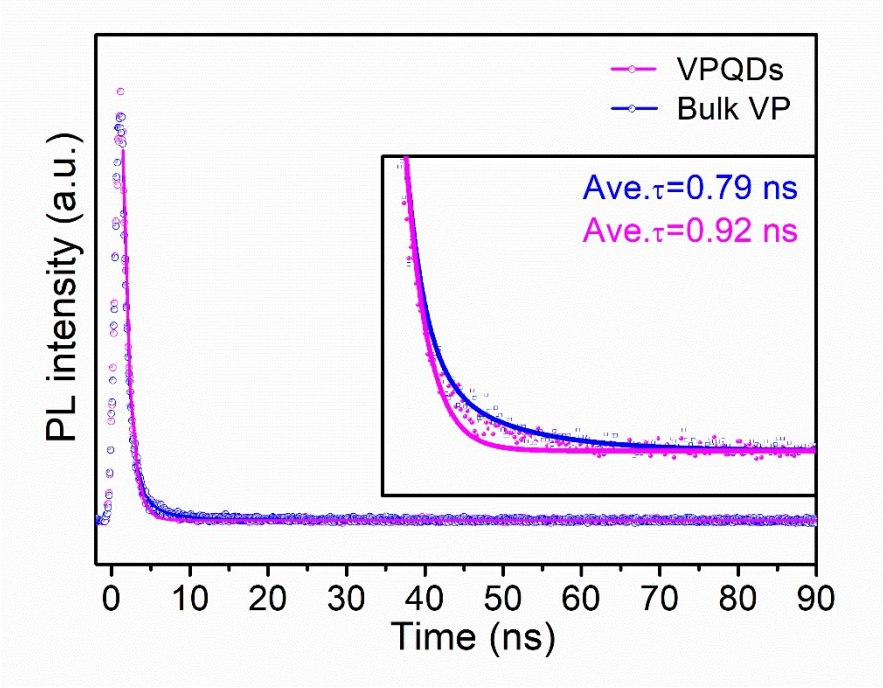

Fig. S10. The corresponding time-resolved PL spectra of VPQDs and the bulk VP crystals.

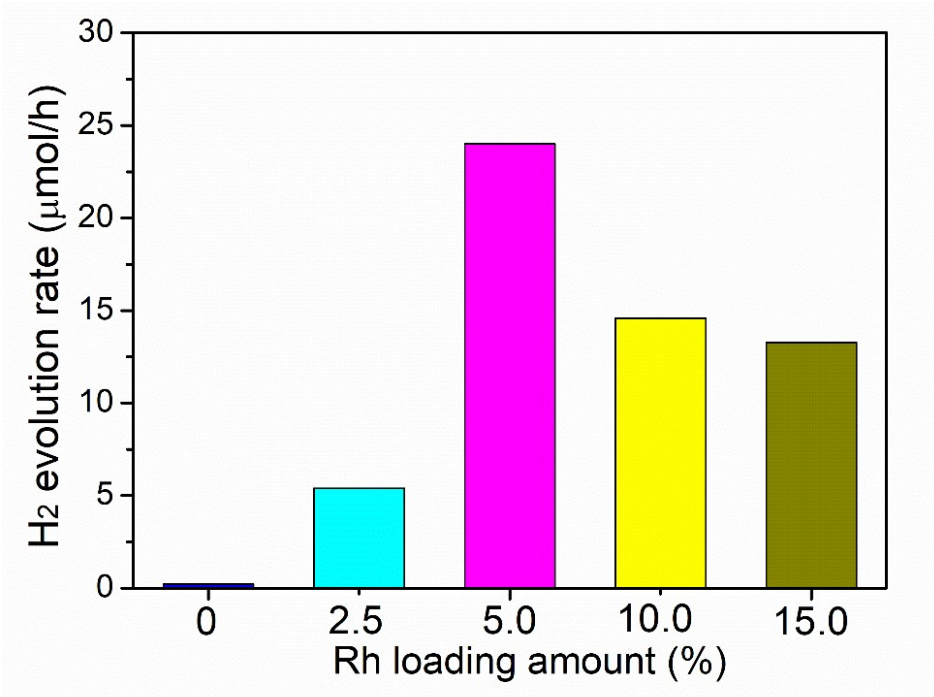

Fig. S11. The effect of the Rh loading amount on the photocatalytic activity of VPQDs obtained at a centrifugation range of 9–11K rpm during H_2 evolution. Photocatalysis parameters: solution: 150 mL aqueous methanol (20 vol%), photocatalyst: 10 mg, light source: 300 W Xe lamp, reaction cell: top-irradiation cell with a Pyrex window.

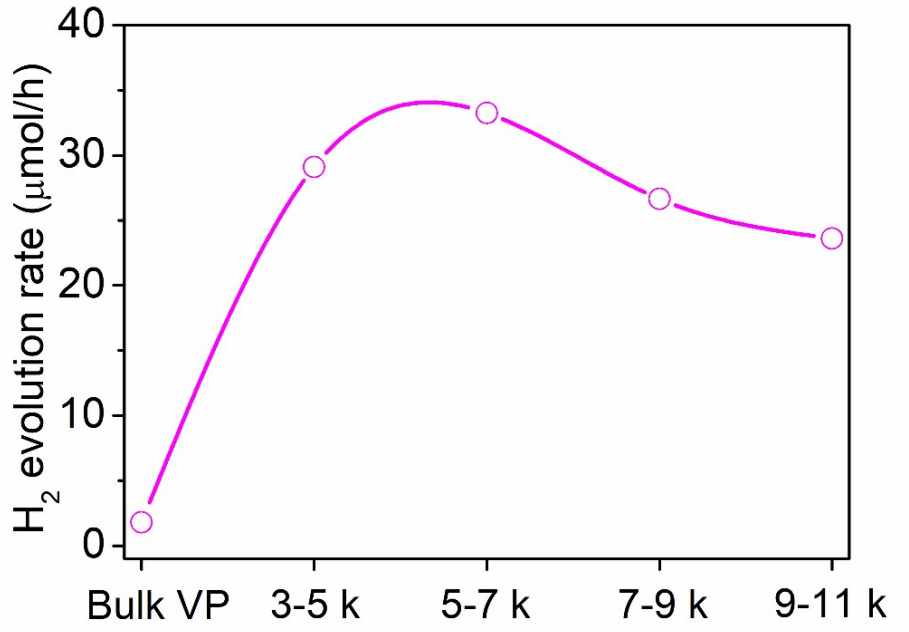

Fig. S12. Photocatalytic H_2 evolution rate over Rh-loaded VPQDs obtained at different centrifugation speeds.

BPQDs:

This synthesis of BPQDs was similar with the synthesis of VPQDs in the Samples Preparation Section. Typically, 20 mg of BP crystals was added in a 50 mL of NMP and treated by a tip sonicator at a power output of 40 W under 5 °C water bath conditions for 6 h. Subsequently, the resulting dispersion was sonicated in an ultrasonic bath continuously for another 5 h. As a result, BPQDs were obtained by centrifuging at 9-11K for 10 min. It was clearly found that the average lateral size of the as-prepared BPQDs is Iin the range of 10-15 nm (Fig. S13).

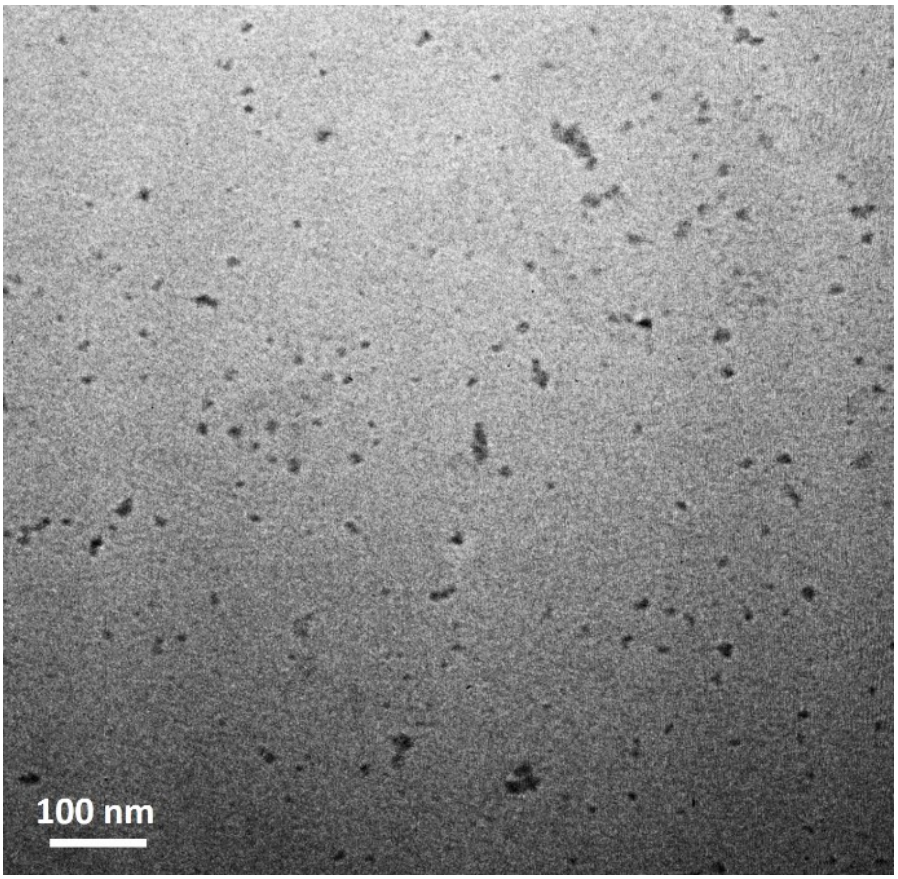

Fig. S13. TEM image of BPQDs.

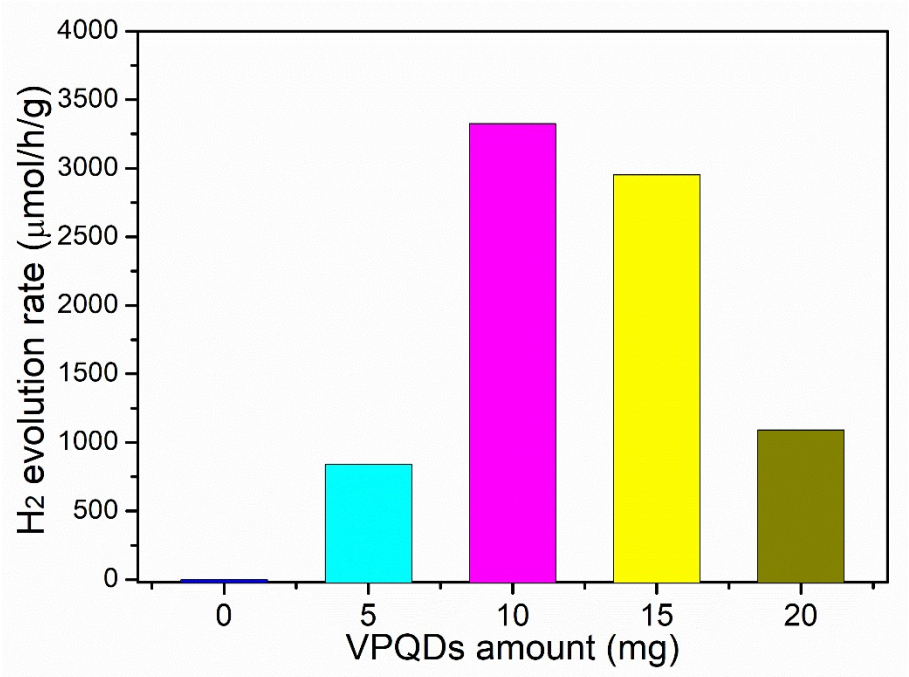

Fig. S14. The effect of the photocatalyst amount on the photocatalytic activity during H_2 evolution using Rh-loaded VPQDs obtained at a centrifugation range of 5–7K rpm. Photocatalysis parameters: solution: 150 mL aqueous methanol (20 vol%), cocatalyst loading amount: Rh, 5 wt%, loading method: $NaBH_4$ reduction, light source: 300W Xe lamp, reaction cell: top-irradiation cell with a Pyrex window.

Table S5. Comparison of photocatalytic H_2 evolution activity of 2D mono-elemental materials.

Photocatalyst	Cocatalyst	Sacrificial agent	Light source	H_2 evolution rate (umol $g^{-1} h^{-1}$)	References
VPQDs	**5 wt% Rh**	**Methanol**	**300W Xe lamp >300 nm**	**3325**	**This work**
VPQDs	**5 wt% Rh**	**Methanol**	**300W Xe lamp >420 nm**	**1862**	**This work**
VP	1 wt% Pt	Methanol	300W Xe lamp >300 nm	675	Chem. Commun. 2022, 58, 12811[10]
BP	2 wt% Ni_2P	TEOA	300W Xe lamp >420 nm	858	Appl. Catal. B, 2019, 242, 422-430[11]
BP	5 wt% Co_3O_4	EDTA	300W Xe lamp >420 nm	420	Angew. Chem. Int. Ed. 2018, 57, 2160-2164[12]
BP	N/A	Na_2S/Na_2SO_3	300W Xe lamp >420 nm	512	Adv. Mater. 2017, 29, 1605776[2]
BP	20 wt% Pt	N/A	300W Xe lamp >420 nm	447	Proc. Natl. Acad. Sci. U. S. A. 2018, 115, 4345-4350[13]
BP	6 wt% P/Co	N/A	300W Xe lamp >420 nm	735	Nat. Commun. 2018, 9, 1397[14]
Crystalline RP	3 wt% Pt	TEOA	300W Xe lamp >420 nm	96	J. Chem. Phys. 2020, 153, 024707[15]
Amorphous RP	3 wt% Pt	TEOA	300W Xe lamp >420 nm	90	Adv. Funct. Mater. 2017, 27, 1703484[16]
Amorphous RP	1 wt% Pt	N/A	300W Xe lamp >420 nm	79	Appl. Catal. B 2022, 312, 121428.[17]
Fibrous RP	Pt	Methanol	300W Xe lamp >420 nm	684	Angew. Chem. Int. Ed. 2016, 55, 9580-9585.[18]
RP	2 wt% Pt	Methanol	300W Xe lamp >420 nm	21	Appl. Catal. B 2021, 297, 120412[19]
RP	0.5 wt% Au	TEOA	300W Xe lamp >420 nm	88	Catal. Commun. 2021, 149, 106197[20]
Dendritic RP	1 wt% Pt	Methanol	300W Xe lamp >420 nm	1280	Appl. Catal. B 2022, 312, 121428[21]
HRP	7.4 wt% Ni	N/A	300W Xe lamp >420 nm	88	Angew. Chem. Int. Ed. 2022, 61, e202204711[22]
Crystalline RP	1 wt% Pt	Methanol	300W Xe lamp >420 nm	1.6	Appl. Catal. B 2012, 111-112, 409-414.[23]
Crystalline Si	N/A	Methanol	300W Xe lamp >420 nm	882	Nat. Commun. 2014, 5, 3605.[24]
α-S	N/A	N/A	300W Xe lamp >420 nm	N/A	J. Am. Chem. Soc. 2012, 134, 9070-9073[25]
Se	N/A	N/A	300W Xe lamp >420 nm	N/A	J. Am. Chem. Soc., 2016, 138, 5206-5209[26]
B	N/A	N/A	300W Xe lamp >420 nm	N/A	Angew. Chem. Int. Ed. 2017, 56, 15506-15518[27]
Sb	N/A	N/A	300W Xe lamp >420 nm	N/A	Adv. Sustainable Syst. 2019, 3, 1800138[28]

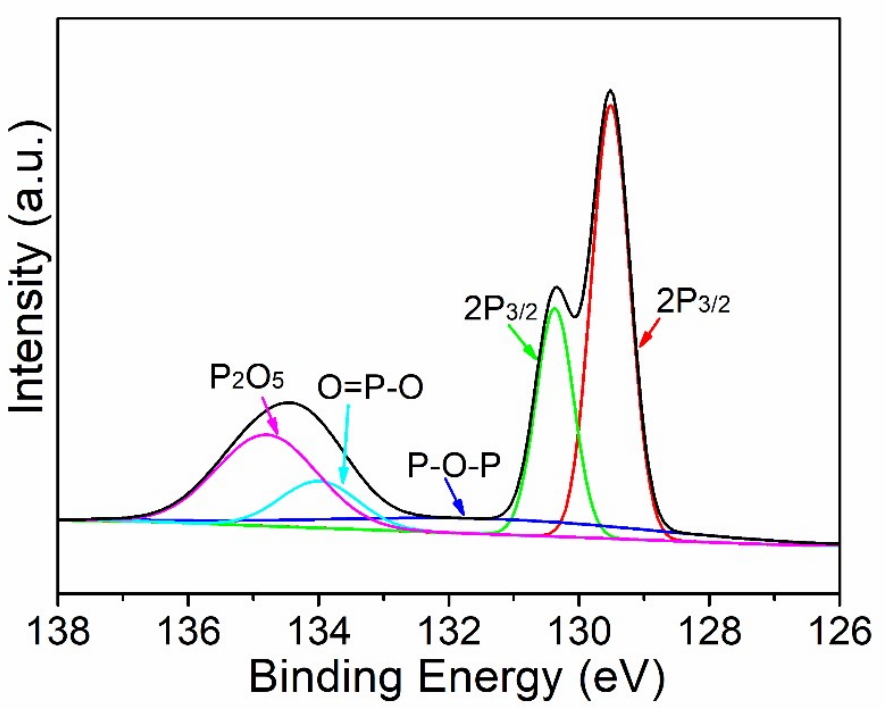

Fig. S15. XPS spectra of VPQDs after reaction.

Table S6. The intensity ratio of P_xO_y to P=P in the XPS spectra of VPQDs before and after reaction.

Samples	P_xO_y	P=P	P_xO_y/P=P
VPQDs (before reaction)	27.7	72.3	0.383
VPQDs (after reaction)	29.6	70.4	0.420

Table S7. Kinetic parameters of TAS decays of bulk VP and VPQDs under 400 nm excitation with time profiles of absorption probed at 500-700 nm.

Samples	τ_1	τ_2	Averageτ
Bulk VP	696.6 ps (69%)	35.6 ps (31%)	681.8 ps

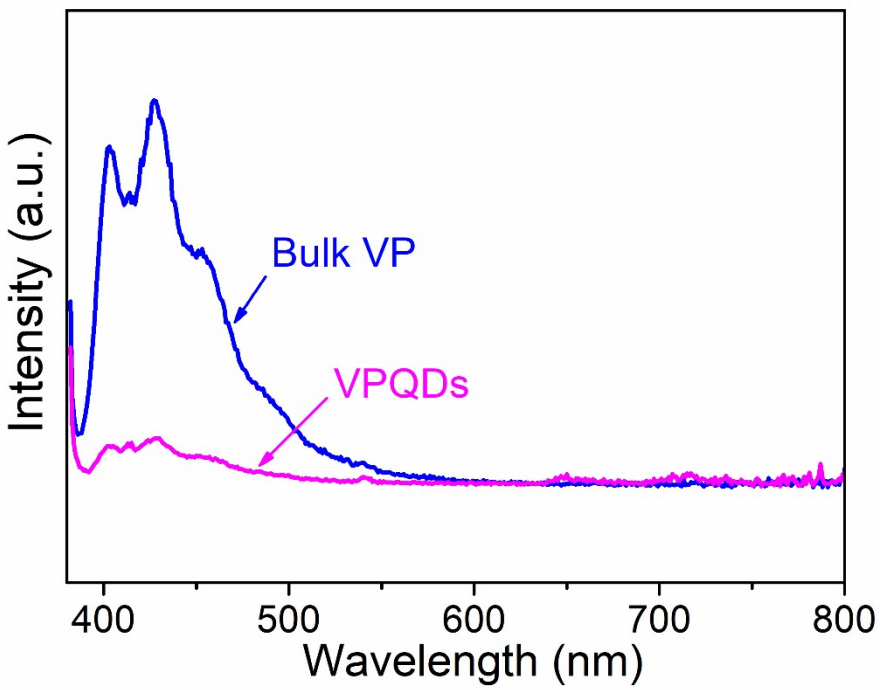

VPQDs	220.9 ps (72%)	14.5 ps (28%)	215.8 ps

Fig. S16. Steady-state PL emission spectra of Rh-loaded VPQDs and the bulk VP crystals.

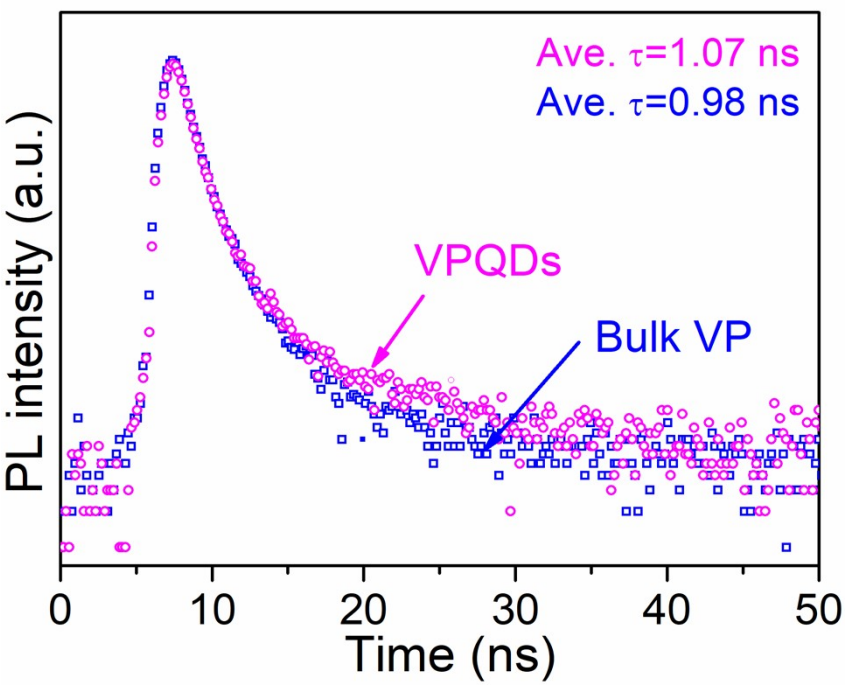

Fig. S17. The corresponding time-resolved PL spectra of Rh-loaded VPQDs and the bulk VP crystals.

References

[1] K. Momma, F. Izumi, *J. Appl. Crystallogr.*, **2011**, 44, 1272–1276.

[2] X. Zhu, T. Zhang, Z. Sun, H. Chen, J. Guan, X. Chen, H. Ji, P. Du, S. Yang, *Adv. Mater.*, **2017**, 29, 1605776.

[3] M. Zhu, S. Kim, L. Mao, M. Fujitsuka, J. Zhang, X. Wang, T. Majima, *J. Am. Chem. Soc.*, **2017**, 139, 13234−13242.

[4] X. Wang, B. Zhou, Y. Zhang, L. Liu, J. Song, R. Hu, J. Qu, *J. Alloys Comp.*, **2018**, 769, 316-324.

[5] R. Zhao, S. Liu, X. Zhao, Y. Cheng, J. Zhang, *Adv. Mater. Interfaces*, **2022**, 2200705.

[6] L. Zhang, H. Huang, Z. Lv, L. Li, M. Gu, X. Zhao, B. Zhang, Y. Cheng, J. Zhang, *ACS Appl. Electron. Mater.*, **2021**, 3, 1043−1049.

[7] R. Zhao, X. Zhao, X. Xu, Y. Zhang, Y. Wang, M. Jin, Z. Liu, Y. Cheng, H.Zheng, J. Zhang, *J. Phys. Chem. Lett.*, **2022**, 13, 35, 8236–8244.

[8] a) F. Liu, R. Shi, Z. Wang, Y. Weng, C. -M. Che, Y. Chen, *Angew. Chem. Int. Ed.*, **2019**, 58, 11791–11795.

[9] Y. Zhu, C. Lv, Z. Yin, J. Ren, X.Yang, C. -L. Dong, H. Liu, R. Cai, Y. -C. Huang, W. Theis, S. Shen, D. Yang, *Angew. Chem. Int. Ed.*, **2020**, 59, 868-873.

[10] M. Gu, L. Zhang, S. Mao, Y. Zou, D. Ma, J. Shi, N. Yang, C. Fu, X. Zhao, X. Xu, Y. Cheng, J. Zhang, *Chem. Commun.*, 2022, **58**, 12811.

[11] R. Boppella, W. Yang, J. Tan, H. -C. Kwon, J. Park, J. Moon, Appl. Catal. B, 2019, 242, 422-430.

[12] M. Zhu, Z. Sun, M. Fujitsuka, T. Majima, *Angew. Chem. Int. Ed.*, **2018**, 57, 2160-2164.

[13] B. Tian, B. Tian, B. Smith, M. C. Scott, Q. Lei, R. Hua, Y. Tian, Y. Liu, *Proc. Natl. Acad. Sci. U. S. A.*, **2018**, 115, 4345-4350

[14] B. Tian, B. Tian, B. Smith, M.C. Scott, R. Hua, Q. Lei, Y. Tian, *Nat. Commun.*, **2018**, 9, 1397.

[15] L. Jing, R. Zhu, Y. H. Ng, Z. Hu, W. Y. Teoh, D. L. Phillips, J. C. Yu, *J. Chem. Phys.*, **2020**, 153, 024707.

[16] L. Jing, R. Zhu, D. L. Phillips, J. C. Yu, *Adv. Funct. Mater.*, **2017**, 27, 1703484.

[17] C. Wu, R. Zhu, W. Y. Teoh, Y. Liu, J. Deng, H. Dai, L. Jing, Y. H. Ng, J. C. Yu, *Appl. Catal. B*, **2022**, 312, 121428.

[18] Z. Hu, L. Yuan, Z. Liu, Z. Shen, J. C. Yu, *Angew. Chem. Int. Ed.*, **2016**, 55, 9580-9585.

[19] S. Li, Y. H. Ng, R. Zhu, S. Lv, C. Wu, Y. Liu, L. Jing, J. Deng, H. Dai, *Appl. Catal. B*, **2021**, 297, 120412.

[20] Q. Cao, M. Guo, J. Cao, H. Lin, S. Chen, *Catal. Commun.*, **2021**, 149, 106197.

[21] C. Wu, R. Zhu, W. Y. Teoh, Y. Liu, J. Deng, H. Dai, L. Jing, Y. H. Ng, J. C. Yu, *Appl. Catal. B*, **2022**, 312, 12142.

[22] M. Wang, S. Xu, Z. Zhou, C. -L. Dong, X. Guo, J -L. Chen, Y. -C. Huang, S. Shen, Y. Chen, L. Guo, C. Burda, *Angew. Chem. Int. Ed.*, **2022**, 61, e2022047.

[23] F. Wang, W. K. H. Ng, J. C. Yu, H. J. Zhu, C. H. Li, L. Zhang, Z. F. Li, Q. Li, *Appl. Catal. B*, **2012**, 111-112, 409-414.

[24] F. Dai, J. Zai, R. Yi, M. L. Gordin, H. Sohn, S. Chen, D. Wang, *Nat. Commun.*, **2014**, 5, 3605.

[25] G. Liu, P. Niu, L. Yin, H. -M. Cheng, *J. Am. Chem. Soc.*, **2012**, 134, 9070-9073.

[26] Y. Kawamata, T. Hashimoto, K. Maruoka, *J. Am. Chem. Soc.*, **2016**, 138, 5206-5209.

[27] Y. Fang, X. Wang, *Angew. Chem. Int. Ed.*, **2017**, 56, 15506-15518.

[28] J. Barrio, C. Gibaja, J. Tzadikov, M. Shalom, F. Zamora, *Adv. Sustainable Syst.*, **2019**, 3, 1800138.